
Article:
Walker, S.N. orcid.org/0000-0002-4105-1547, Balikhin, M.A., Gedalin, M. et al. (2 more authors) (2021) Small scale magnetic structures: Cluster observations. Journal of Geophysical Research: Space Physics, 126 (10). e2021JA029674. ISSN 2169-9402

https://doi.org/10.1029/2021ja029674

JGR Space Physics

RESEARCH ARTICLE
10.1029/2021JA029674

Special Section:
Cluster 20th anniversary: results from the first 3D mission

Small-Scale Magnetic Structures: Cluster Observations

Simon N. Walker[1], Michael A. Balikhin[1], Michael Gedalin[2], Patrick Canu[3], and Keith H. Yearby[1]

[1]Automatic Control and Systems Engineering, University of Sheffield, Sheffield, UK, [2]Department of Physics, Ben-Gurion University, Beer-Sheva, Israel, [3]Laboratoire de Physique des Plasmas, CNRS/Ecole Polytechnique/Obs. de Paris/UPMC/Univ. Paris-Sud, Palaiseau, France

Key Points:

- Cluster STAFF-SC magnetometer observations of previously unreported nonlinear structures in the inner magnetosphere are presented
- The small separation of two of the Cluster satellites enables their spatial and temporal properties to be investigated
- We argue that these structures can be generated by thin current filaments whose size is a few tens of kilometers

Correspondence to:
S. N. Walker,
simon.walker@sheffield.ac.uk

Citation:
Walker, S. N., Balikhin, M. A., Gedalin, M., Canu, P., & Yearby, K. H. (2021). Small-scale magnetic structures: Cluster observations. *Journal of Geophysical Research: Space Physics*, *126*, e2021JA029674. https://doi.org/10.1029/2021JA029674

Received 14 JUN 2021
Accepted 30 AUG 2021

Abstract Within the inner magnetosphere, the occurrence of plasma waves and/or magnetic field structures plays an important role in the dynamics of the particle populations, accelerating some particles to higher energies while scattering others. The 2013 Cluster Inner Magnetosphere Campaign was designed to investigate this process based on observations made at small separation scales. In addition, it provides an ideal opportunity for the study of small-scale structures. This paper presents observations of previously unreported small-scale magnetic field structures and investigates their characteristics and spatial properties. These structures, seen in the STAFF-SC data set, are characterized by a rotation in the field direction and are observed to have spatial sizes of a few tens of kilometers, with a central core region around 10 km and are probably filamentary current structures. Using a variance analysis, it was determined that the maximum variance direction was close to being perpendicular to the external magnetic field. Based on the size of the central core region the current density is of the order of 10–40 nAm^{-2}. While they may affect the profile of these structures, data calibration effects were ruled out as their origin.

1. Introduction

Within the terrestrial inner magnetosphere, plasma wave modes play a key role in the redistribution of energy between the various particle populations present, through processes such as acceleration or scattering. During the period July-October 2013, Cluster instigated a special Inner Magnetosphere Campaign (IMC) whose primary objectives were to investigate the relationship between plasma wave modes and changes in the particle distributions. These data enabled the investigation of the origin (Balikhin et al., 2015), dispersion relation (Walker et al., 2015), propagation (Shklyar & Balikhin, 2017), and structure (Aryan et al., 2019) of magnetosonic waves. The small-scale separations (a few tens of kilometers) achieved also enable the examination of the spatiotemporal properties of any small-scale structures observed.

During this campaign, it was noted that some of the observational periods exhibited small-scale nonlinear magnetic field measurements from the Cluster STAFF-SC search coil magnetometer that, to our knowledge, have not been reported previously. These magnetic field structures have some analogies with other commonly observed small-scale structures. For example, the appearance of these structures is reminiscent of the electric field associated with electron/ion holes. However, while these distinctive magnetic structures were observed, there appears to be no counterpart in the electric field.

In this paper, the spatiotemporal nature of these nonlinear phenomena is investigated using data primarily collected during the Cluster IMC. This paper is structured as follows. Section 2 presents observations from the Cluster satellites, Section 3 describes two such events in more detail using single satellite measurements, Section 4 compares measurements made on two closely separated satellites. Section 5 provides an interpretation of the observations.

2. Data and Instrumentation

In this section, some typical examples of observations of these structures are presented. The measurements were made by the satellites Cluster 3 and Cluster 4 (Escoubet et al., 1997) as they traversed the inner magnetosphere. Similar observations were made by Cluster 1 and Cluster 2. However, their separations (~300 km for Cluster 1 to Clusters 3 and 4 while Cluster 2 is ~4,500 km distant) mean that it is virtually impossible

to be certain that two satellites observe the same structure. The Cluster satellites have an eccentric 57 h, polar orbit with apogee of 18.7 R_E, perigee 3 R_E, and spin rate of ~15 rpm. The data used in this study come primarily from the SpatioTemporal Analysis of Fields and Fluctuations search coil magnetometer (STAFF-SC) (Cornilleau-Wehrlin et al., 1997) (instrument https://doi.org/10.5270/esa-yrzyijm). The STAFF-SC Calibrated Waveform (CWF) data set in GSE coordinates is used. This data set provides waveform measurements of magnetic fluctuations relative to the background field over the frequency range 0.6–180 Hz with a sensitivity of 10^{-7} nT^2Hz^{-1} at 10 Hz. These measurements are supported by observations from the fluxgate magnetometer (FGM) (Balogh et al., 1997) (instrument https://doi.org/10.5270/esa-hxcrsz5), the Electric Fields and Waves instrument (EFW) (Gustafsson et al., 1997) (instrument https://doi.org/10.5270/esa-jti-98hx), the Waves of High frequency and Sounder for Probing of Electron density by Relaxation instrument (WHISPER) (Décréau et al., 1997) (instrument https://doi.org/10.5270/esa-6stdo07), and the Wideband instrument (WBD) (Gurnett et al., 1997) (instrument https://doi.org/10.5270/esa-h8ck8ox) that measures one component of the spin plane electric field. Collectively, the Cluster Wave Experiment Consortium (WEC) instruments are centrally coordinated and controlled by the Digital Wave Processor (DWP) (Woolliscroft et al., 1997) (instrument https://doi.org/10.5270/esa-ftdfdba). All data used in this study were obtained from the Cluster Science Archive (https://csa.esac.esa.int/csa-web/). Unfortunately, there are no particle moments available from PEACE and CIS-CODIF on Cluster 4 was operating in a magnetospheric mode with a lower energy cut-off of ~25 eV/e and so misses the majority of the cold plasma that exists within the plasmasphere, and the plasma frequency was too high to be recorded during active soundings by WHISPER and so there are no reliable density measurements during this period.

The observations presented here were made on July 2, 2013 between 05:28 and 05:44 UT. The Cluster spacecraft were operating in Burst Science Mode 2 (BM2) in which STAFF-SC data were sampled at 450 samples/s, FGM at 22 samples/s. WBD was operating in baseband with a bandwidth of 9.5 kHz, sampled at 27 ksamples/s and decimated by a factor of 4 to enable them to be inserted into the normal Cluster telemetry system. In BM2, WBD and WHISPER share the telemetry allocation and therefore their signals are not continuous.

During this period of observations, Cluster 3 was located at (2.53, 1.85, −0.60) R_e (GSM), MLT 14.75 h and within 5° of the magnetic equator in the dayside inner magnetosphere, just after passing through perigee (04:55 UT) on its polar orbit and crossed the magnetic equator from north to south at around 05:36 UT. WHISPER observations show that the satellites were in the plasmasphere during the period under study. The separation between Cluster 3 and Cluster 4 was $S \approx (2.5, 26.5, 43.9)$ km (GSM), $|S| \approx 51.3$ km, and both satellites were traveling at a velocity $V \approx (2.7, -1.9, -4.7)$ kms^{-1} (GSM), $|V| \approx 5.78$ kms^{-1} with Cluster 3 leading along the orbital track. The closest approach of the track of Cluster 4 to that of Cluster 3 would be around 27 km after a delay of some 7.6 s. By comparing measurements from Cluster 3 and Cluster 4, it should be possible to determine if both satellites see the same structure and to estimate the spatial extent of these structures.

Figure 1 shows examples of the magnetic structures observed by the Cluster 3 (blue) and Cluster 4 (red) STAFF-SC search coil magnetometers. All panels show the magnitude of the STAFF-SC magnetic field ($|B|$ in nT). Panel (a) shows an overview of a 7 min period between 05:30 and 05:37 UT. It can be seen that on many occasions within this period the amplitudes exhibit short lived spikes with typical magnitudes in excess of 0.1 nT. This compares to a background field strength of ~1,000 nT, i.e., $dB/B_0 \approx 1 \times 10^{-4}$. Panels (b–d) show the STAFF-SC magnetic field profile of some of these localized magnetic field spikes in greater detail.

Panels (b) and (c) of Figure 1 display the type of events that occur most commonly in this data set. These events are characterized by the occurrence of two peaks in the magnitude of the field with amplitudes typically in the range 0.05–0.2 nT and appear to be spatially isolated since the field either side shows no other strong features. Panel (b) shows two magnetic field structures, one observed by Cluster 3 (blue), the other Cluster 4 (red). Both sets of observations show two large peaks with $|B| > 0.1$ nT, separated by a narrow region in which the field drops to around zero. This whole structure passes over the individual spacecraft in less than 850 ms. Panel (c) shows a similar bipeaked structure, observed by Cluster 3 alone. In this case, the peaks are lower in amplitude and the central minimum is not as pronounced. In both Panels (b) and (c), the events appear fairly symmetrical around the central minimum since the peaks have similar amplitudes and durations.

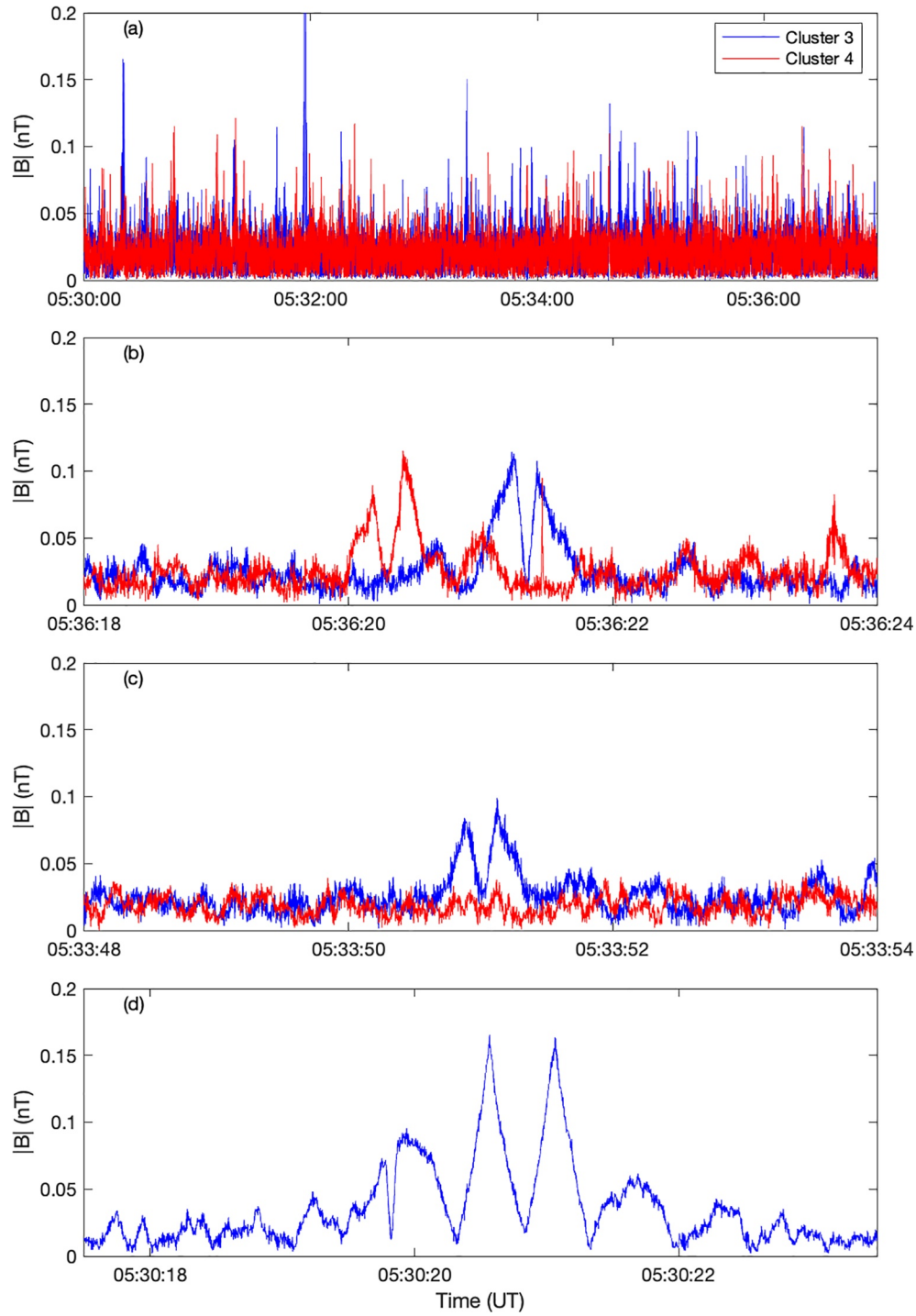

Figure 1. Examples of the spike-like magnetic field observations from the STAFF-SC magnetometer onboard Cluster 3 (blue) and Cluster 4 (red) on July 2, 2013.

Panel (d) shows an example of an event in which four peaks with amplitudes ≥0.07 nT are observed in close proximity by Cluster 3. This event may consist of two individual, unrelated structures such as those shown in Panels (b) and (c) or may possibly be two crossings of the same event. The first pair of peaks are quite asymmetric around the narrow central minimum that divides them with the first peak exhibiting a lower amplitude and shorter duration. In contrast, the second pair of peaks exhibit larger amplitudes, with a symmetrical appearance, and are separated by a wide field minimum.

When analyzing data from a single spacecraft, these features in the STAFF-SC magnetic field may appear be due to some form of interference in the waveform or calibration effect. However, as shown in Panel (b), similar features are observed by two different satellites. While these events are typically only observed by a single satellite (as shown in Panel c), Panel (b) presents an example in which both Cluster 3 and Cluster 4 observe similar structures within a second of each other. Thus, it appears that these events are observations of real structures rather than due to some interference effect. Possible calibration effects are discussed further in Section 5.

Henceforth, these features are referred to as bipolar magnetic structures (BMS). In Sections 3 and 4, we take a closer look at the structure of the magnetic fields within these BMS using both single and dual spacecraft measurements.

3. Single Satellite Observations

3.1. Event 1: July 2, 2013 05:36:21

Figure 2 shows the magnetic field observations made by STAFF-SC on C3 between 05:36:20 and 05:36:22 UT. Panel (a) shows the magnitude of the magnetic field while panels (b–d) show the GSE field components. Panel (e) shows the magnitude of the background magnetic field measured by FGM and Panel (f) the WBD electric field.

During this period, a BMS was observed in the STAFF-SC magnetic field magnitude, centered around 05:36:21.4 UT. The field magnitude (Panel a) increases from a minimum of 0.015 nT to a peak value of 0.11 nT. At this point the field strength quickly reduces to a local minima of 0.005 nT in the central region before increasing to a second peak of 0.10 nT. Following the second peak, the field decays away to background levels, similar to those encountered prior to the event. The whole BMS was crossed in around 0.8 s.

The B_X (Panel b) and B_Y (Panel c) components show that, as the BMS was crossed, the STAFF-SC magnetic field direction undergoes a clear three stage rotation. In the first stage, as the magnetic field strength changes from the background level to the first peak, the field changes to a more antisunward and dawn-ward direction. In the center, between the peaks, the field exhibits a rapid rotation through ∼160° before returning back, almost to its original direction as the field strength decays. The B_Z component remains around zero throughout the event.

Comparing the STAFF-SC wavefield (Panel a) to the background magnetic field determined by FGM (Panel e), it is observed that throughout the period of the crossing of this BMS the background field exhibits small jumps of the order 0.4 nT. These variations superficially resemble interference fringes are an artifact of the 0.5 nT quantization of each component of the raw data, and their changing contribution to the total field as the spacecraft rotates. The fluctuations seen by STAFF-SC are too small to be visible by FGM. Since the magnetometers use different techniques to measure the same field it appears that the field associated with the BMS is roughly perpendicular to the background magnetic field. On comparing the FGM and STAFF-SC measurements during the period of the BMS central region, these fields are perpendicular to each other. This conclusion is investigated further below using variance analysis.

Panel (f) shows the WBD electric field. At this time, the attitude of the Cluster 3 implies that the spin plane is nearly perpendicular to the background magnetic field direction. As a result, the angle between the electric field antenna and background magnetic field varies in the range 80–100° so that the WBD data correspond to the perpendicular electric field component ($E_\perp$). The maximum amplitude of this electric field component is $\left|E_\perp\right| < 0.2\,\mathrm{mV\,m^{-1}}$ and this amplitude is similar before, during, and after the structure is observed. Likewise, the electric field and spacecraft potential measurements from EFW (not shown) exhibit no obvious changes in their characteristics as this structure is encountered. Thus, it appears that there are no large electric fields to be associated with this structure.

In order to investigate the orientation of the structure, a variance analysis (Sonnerup & Cahill, 1967) of the STAFF-SC field observed within the structure was performed. To remove some of the high frequency noise, a three-point average was applied to the data set. Figure 3 shows a hodogram of the Cluster 3 STAFF-SC magnetic field components rotated into the variance reference frame. Panel (a) displays the minimum v maximum variance components, panel (b) maximum v intermediate, and panel (c) the minimum

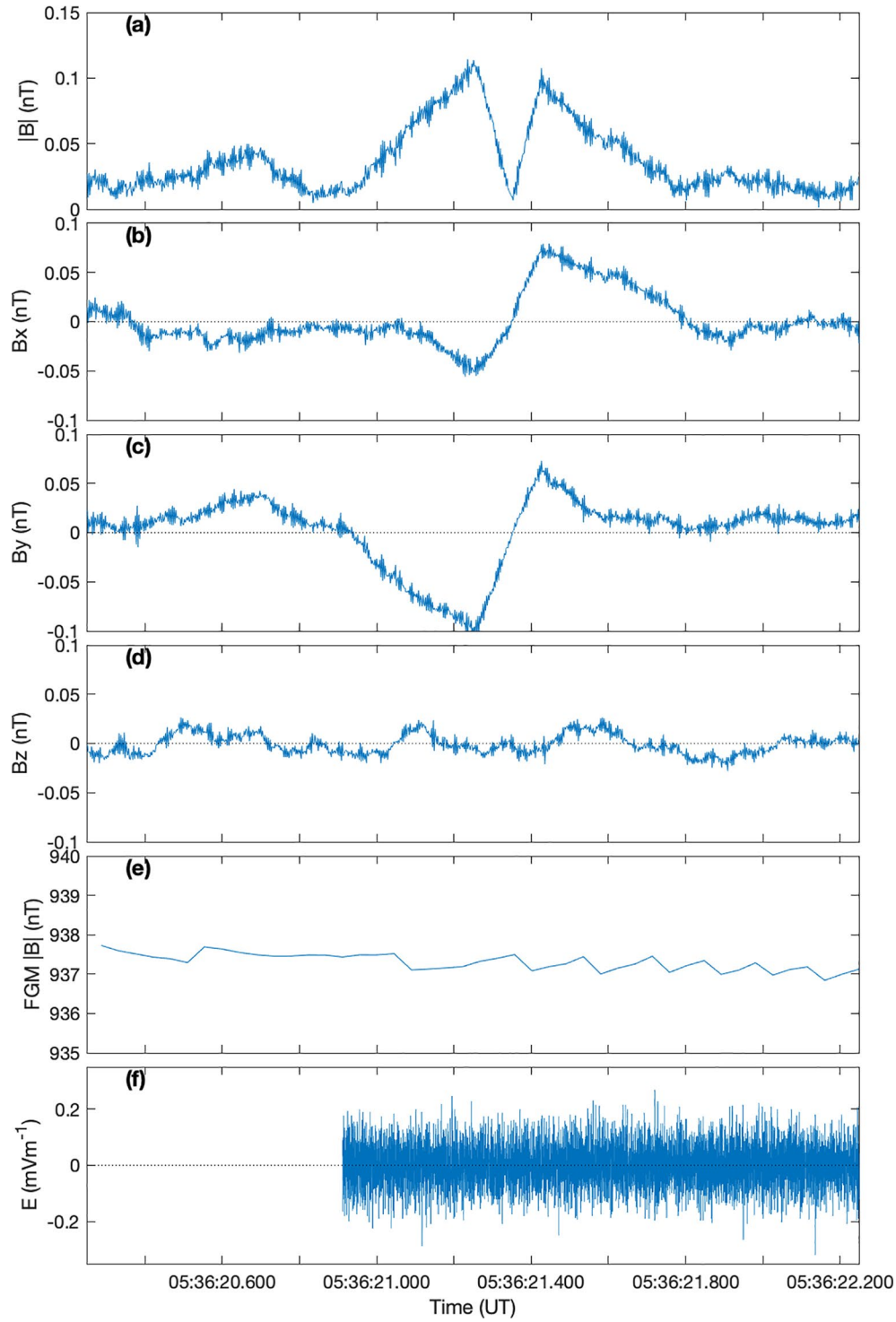

Figure 2. A comparison of the STAFF-SC field magnitude and GSE components, FGM magnetic field magnitude and WBD electric field observations made by Cluster 3 on July 2, 2013 between 05:36:20.3 and 05:36:22.2 UT.

v intermediate. Panel (d) shows the magnitude (black) and variance frame components (red—maximum, green—intermediate, and blue—minimum) of the magnetic field.

The ratios of the eigenvalues were $\lambda_{Max}/\lambda_{Int} \approx 20, \lambda_{Int}/\lambda_{Min} \approx 6.5$ indicating that the maximum variance direction is well defined with errors (Khrabrov & Sonnerup, 1998) of <1° and ≈10° in the maximum and

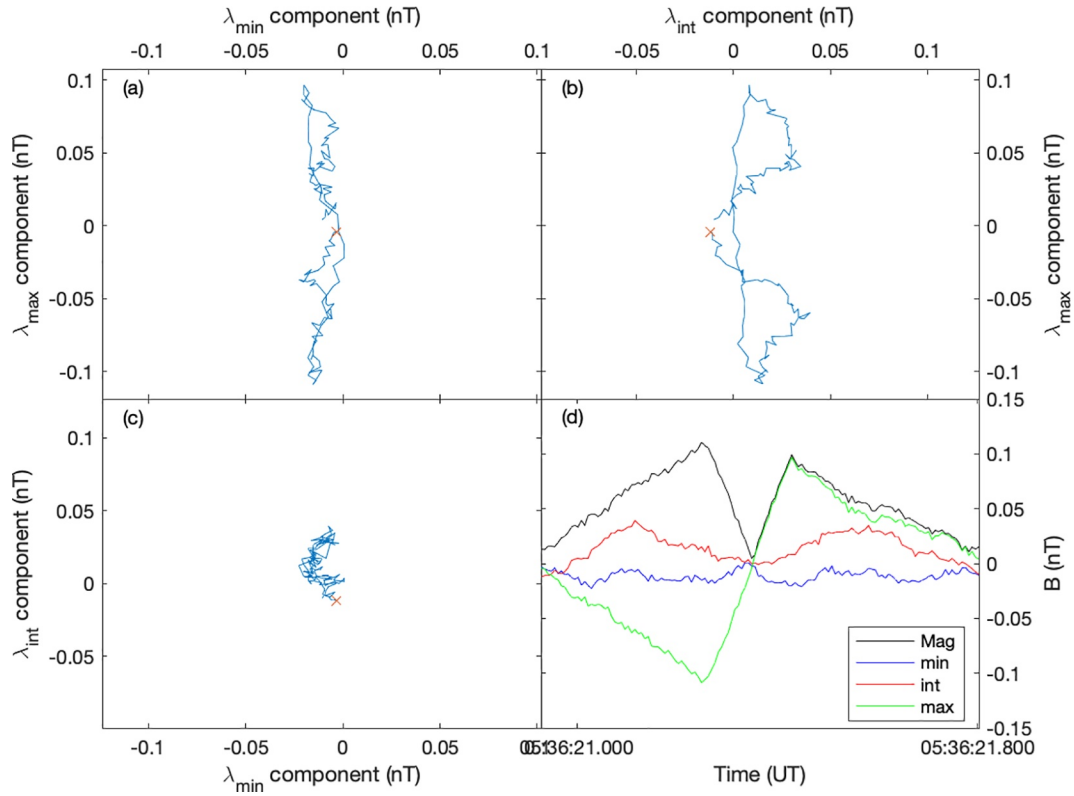

Figure 3. Hodogram of the magnetic field components in the variance reference frame. The red cross indicates the start point of the trace.

minimum variance directions respectfully. The maximum variance direction lies almost perpendicular to the background magnetic field, $\Theta_{\lambda_{max}B} \sim 85°$, indicating that the majority of the field rotation occurs in the plane perpendicular to the background field, while the angle between the minimum variance direction background field was ~60°.

Panel (d) of Figure 3 shows the components of the STAFF magnetic field rotated into the variance reference frame. The black line represents the magnitude of the magnetic field $|B|$. The maximum variance component is shown in green, the intermediate in red, and the minimum in blue. It is clearly seen that the maximum variance component follows the overall magnitude very closely throughout the structure, especially so in the region of the central field minima, and its sense changes from negative during the first peak to positive within the second peak. The intermediate component is greatest in the regions flanking the center of the structure during which the initial (and final) gradual field rotations were observed and decreases to zero during the central minimum. The minimum variance component is nonzero throughout the structure except during the period when the central minimum was observed.

3.2. Event 2: July 2, 2013 05:31:19

A second BMS, encountered between 05:31:18.5 and 05:31:20.3 UT by Cluster 3, is shown in Figure 4 (using the same format as Figure 2). This event differs from that presented above in that there are four peaks in the STAFF-SC field magnitude, each pair being associated with a different rotation in direction of the STAFF-SC magnetic field. The first pair of peaks differ in magnitude, with the first (0.054 nT) being just over half the size of the second (0.092 nT). These peaks are separated by a local minimum in the field that corresponds to a field rotation that occurred primarily in the B_Y component as seen from Panel (c). Between the second and third peaks the field rotates slowly back toward the direction it displayed prior to the first structure with a brief pause before continuing passed its initial direction, as evidenced in both the By and Bx GSE components. In contrast to the first pair of peaks, the second pair are observed with similar magnitudes of

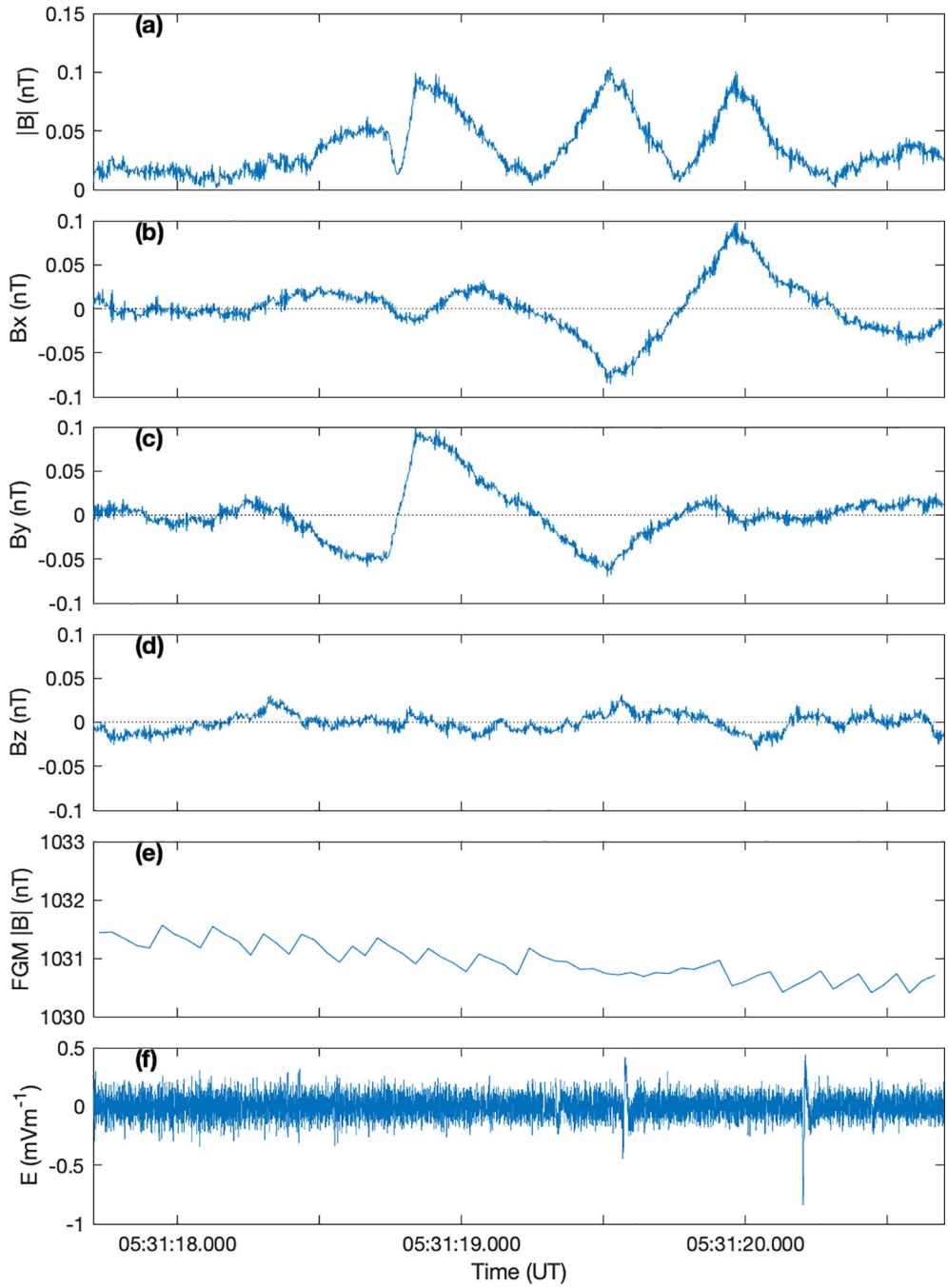

Figure 4. The STAFF-SC field magnitude and GSE components, FGM magnetic field magnitude and WBD electric field observations made by Cluster 3 on July 2, 2013 between 05:31:17.5 and 05:31:20.75 UT.

0.098 and 0.090 nT. The associated field rotation between these peaks occurs mainly in the B_X component, with a minor contribution by B_Y. This rotation is not as monotonic as that observed between the previous pair of peaks and takes place over a longer time period. Panel (e) shows that, once again, there appears to be no feature associated with either structure in the background magnetic field measured by FGM. WBD electric field measurements are shown in Panel (f). It should be noted that the data plotted here differ from those obtained online because they have been recalibrated. The short period (milliseconds) bipolar features seen in this data are an artifact of changes in the instrument gain. In similarity with the first event discussed

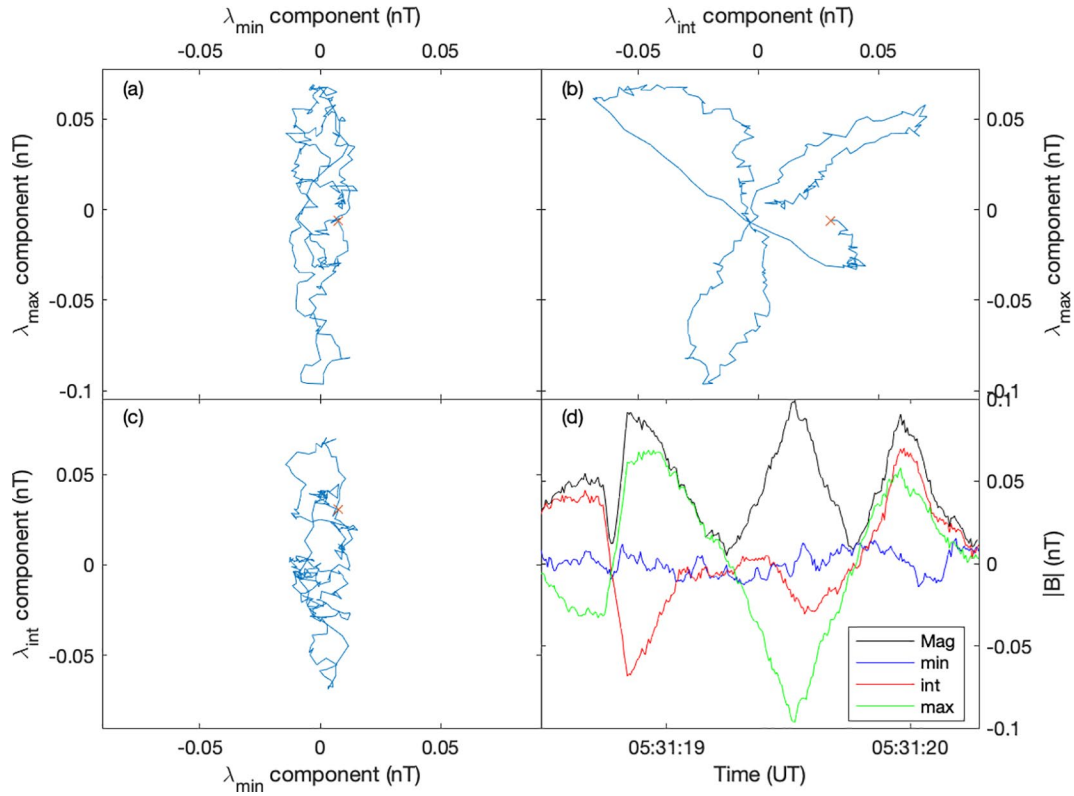

Figure 5. Hodogram of the magnetic field components in the variance reference frame.

above the maximum in the electric field component measured was around 0.2 $\mathrm{mV\,m^{-1}}$ and there appears to be no specific features related to the BMS.

Are these structures actually somehow related or is this an observation of two BMS occurring one after the other? Judging from the profiles alone, this event probably consists of two unrelated structures. To shed further light on this question we perform a variance analysis to compare their individual and combined orientations.

A variance analysis, based on the period encompassing both structures, reveals a well-defined minimum variance direction ($\lambda_{Int}/\lambda_{Min} \approx 19$) while $\lambda_{Max}/\lambda_{Int} \approx 2$. Figure 5 shows a hodogram of the magnetic field components rotated into this variance frame using the same format as Figure 3. The maximum versus minimum and intermediate versus minimum components (panels a and c) exhibit a fairly linear relationship throughout this event where as the maximum versus intermediate components (panel b) shows a clockwise rotation of the field with each peak extending the envelope in a different direction, resulting in a propeller shaped trace. This shows that the field rotation observed between the first and second peaks and the third and fourth occur in almost perpendicular directions. The minimum variance eigenvector direction was found to be close (within 15°) to that of the background magnetic field and so the intermediate and maximum variance directions lie mainly in the plane perpendicular to the background field.

Panel (d) of Figure 5 shows the variance frame components and magnitude of the magnetic field based on the variance frame determined over the whole event. This panel clearly shows that this reference frame does not resolve the variance components in a consistent manner. While the minimum variance component is the smallest throughout this event, it is seen that the intermediate component is the largest for peaks 2 and 4 which would not be expected if the event were comprised of one structure.

However, if these four peaks are analyzed as two pairs i.e., between 05:31:18.48 and 05:31:19.25 (peaks 1 and 2), and 05:31:19.25 to 05:31:20.28 (peaks 3 and 4) it is found that in both cases $\lambda_{Int}/\lambda_{Min} < 5$ while $\lambda_{Max}/\lambda_{Int} > 15$. This apparent contradiction with the result presented above can be explained by the fact

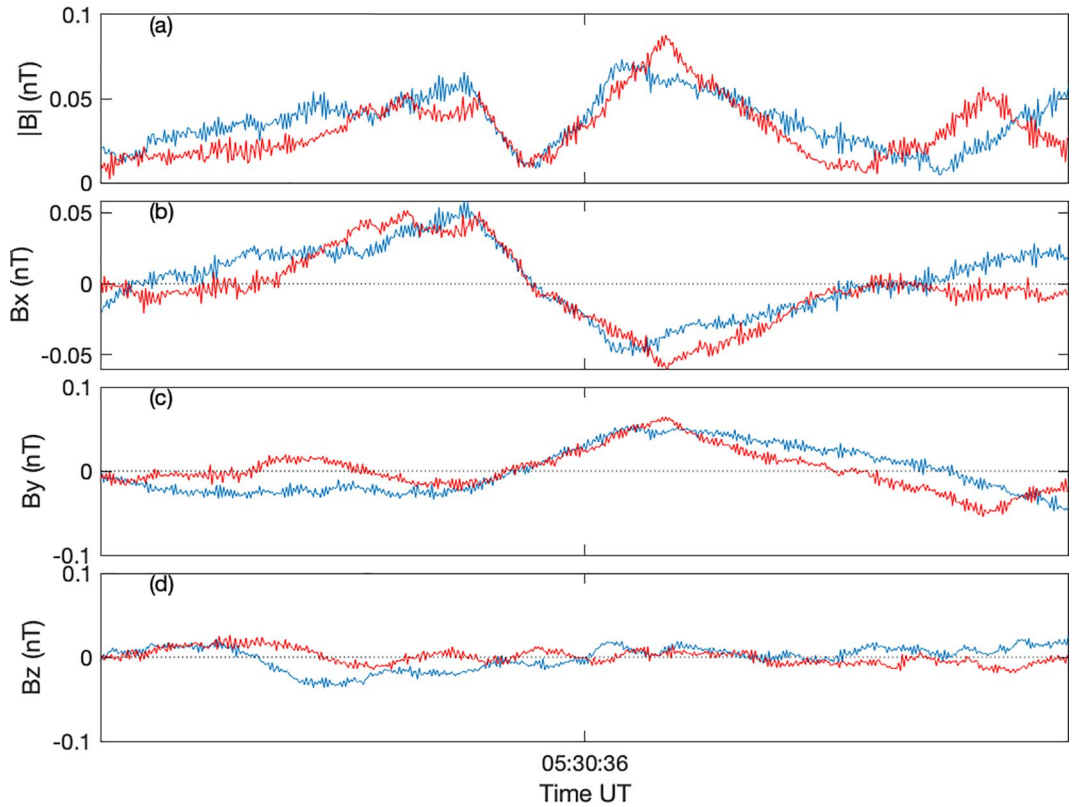

Figure 6. A comparison of the STAFF-SC magnetic field magnitude and GSE components measurements by Cluster 3 (blue) and Cluster 4 (red). Note that a time offset of 3.913 s has been added to the Cluster 3 measurements to align the structures.

that the minimum variance directions differ by ~20° whereas the maximum variance directions differ by > 70°. Thus, it appears that this event consists of two BMS that happened to be observed one after the other.

4. Dual Satellite Observations

The observations discussed in Section 3.1 and 3.2 are from one spacecraft, namely Cluster 3. On some occasions, the same structure may be observed by Cluster 4. Using dual satellite observations, it is possible to estimate the spatial size of these structures and the velocity at which they move.

4.1. Comparison of Cluster 3 and Cluster 4 Observations July 2, 2013 05:30:36

The first example of a structure observed by both Cluster 3 and Cluster 4 is shown in Figure 6. Panel (a) shows the STAFF-SC magnetic field magnitude while Panels (b–d) show the *X*, *Y*, and *Z* GSE field components, respectively. A time offset of 3.191 s has been added to the Cluster 3 measurement so that the two observations are aligned.

The magnetic field profile observed by Cluster 3 is very similar to that observed by Cluster 4. Both satellites see similar profiles of the central minimum, in which the field magnitude drops to ~0.011 nT with similar rates of change on either side. Both satellites observe that this minimum is associated with a field rotation primarily observed in the GSE *XY* plane. The profiles of the B_X and B_Y components are the same on both spacecraft, i.e., the main rotation is seen in the B_X component as a change in the field from positive to negative while both B_Y components change negative to positive. The B_Z field component remaining stable throughout the passage of the structure passed both satellites. The field peaks either side of the minimum do differ in profile, which may be evidence of the evolution of the structure, either spatially, temporally, or both between the two satellite passes.

Are these BMS planar structures? To investigate this question a variance analysis was performed on the STAFF-SC measurements from Cluster 3 and Cluster 4. For both BMS, the ratios of the eigenvalues indicate that the maximum variance direction is well defined, in similarity with the events discussed above. However, the orientation of the two variance frames differs significantly. The minimum variance directions differ by ~60° and the maximum variance directions by ~80°. This difference implies that these BMS are nonplanar in nature, i.e., these magnetic field signatures are probably not the result of the satellites encountering a current sheet. Instead, it looks as if the satellites encountered some form of current filament. The possible structure associated with these BMS events will be discussed further in Section 5.

In order to determine the approximate scale of these structures it is assumed that they are current filaments that are aligned with the local magnetic field. As a result, it is possible to estimate their motion in the plane perpendicular to the external magnetic field using two-point observations. The separation vector between the two spatial locations at which the BMS was observed by Cluster 3 and Cluster 4 was $S = (12.0, 18.0, 23.9)$ km (GSM), $|S| \approx 32.25$ km, making an angle of ~47° with the background magnetic field. Thus, the separation of the observation points in the direction perpendicular to the background magnetic field is 23.7 km. The time delay between the two satellites observing the BMS was ~3.9 s, resulting in a velocity of 12 kms^{-1} in the satellite frame.

Based upon this propagation velocity perpendicular to the background magnetic field the size of the structure may be estimated. To cross the whole BMS, Cluster 3 took 0.96 s while Cluster 4 took 0.89 s, corresponding to a distance of around 12 km. While the region of the central magnetic field minimum was crossed in 0.18 s, a distance of 2.5 km. Without reliable density measurements the ion and electron inertial lengths cannot be calculated. However, if it is assumed that the density in the plasmasphere is of the order of 100 cm^3, the resulting ion inertial length would be around 23 km. Thus, the spatial extent of the whole BMS appears to be less than an ion inertial length.

4.2. Comparison of Cluster 3 and Cluster 4 Observations July 2, 2013 05:36:21

Figure 7 shows a second structure that was observed by both Cluster 3 and Cluster 4 using the same format as Figure 6. The data from Cluster 3 have been discussed in detail in Section 3.1. In this case, Cluster 4 observes the structure first and so Cluster 3 measurements have been shifted by −1.065 s so that they align with those of Cluster 4.

Both satellites observe a clear two peaked structure in the STAFF-SC magnetic field magnitude (Panel a). However, in the case of this particular structure their profiles differ quite markedly. While Cluster 3 (blue) exhibits a symmetrical structure, the peaks observed by Cluster 4 differ in both magnitude and profile. The profile of the central minimum also differs. Cluster 3 observes a symmetrical change in the field and a monotonic decrease and increase in the field magnitude, Cluster 4 data show a two stage decrease and increase with the steepest changes observed in the outer regions of the central minimum. The field rotation associated with this central minimum also show significant difference between the two satellite measurements. Both satellites show very little change in the B_Z component. The B_X transition on both satellites exhibit the same profile with an initial antisunward rotation, followed by a sunward rotation through the central minimum. In contrast, the B_Y components vary in different directions with Cluster 3 observing a negative deviation as the fields build up to their peak and a sharp positive deviation within the central minimum while Cluster 4 sees a deflection in the opposite direction. This would indicate that the structure is not planar, and provides further evidence that these structures appear to be some form of current filament. The differences in the appearance of the B_Y component could be explained if the satellites cross the structure on opposite sides of the central axis of the filament.

Comparing the variance frames calculated separately for Cluster 3 and Cluster 4, it was found that both frames possessed a well-defined maximum variance direction and that these directions differed by ~16°. However, the intermediate and minimum variance directions differ by around 70°. Thus, it appears that these BNS are not planar in nature.

As noted in the discussion above, this structure is first observed by Cluster 4 and then by Cluster 3 after a time delay of around 1.06 s. The locations of the satellites differ by 57 km at the point of observation and directed at an angle of 145° to the local magnetic field. Therefore, the two observation points are separated

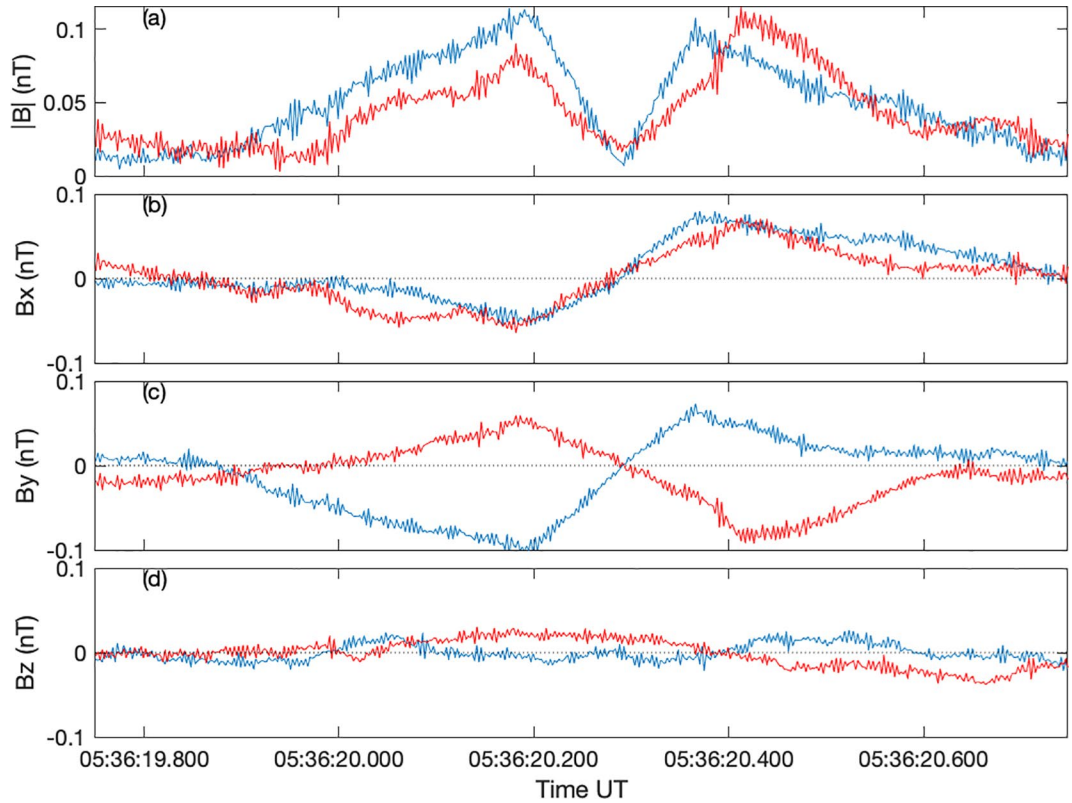

Figure 7. A comparison of the STAFF-SC magnetic field magnitude and GSE components observed by Cluster 3 (blue) and Cluster 4 (red).

by 51 km in the direction perpendicular to the local magnetic field. Thus, the BMS appears to propagate at ~48 kms^{-1}. Cluster 3 crossed the whole BMS in 0.85 s, with the core crossing taking 0.17 s. Thus, the size of the whole structure and core region are approximately 40 and 8.3 km, respectively. Again, based on an estimated plasmasphere density of 100 cm^{-3}, the spatial size of the whole BMS is of the order of an ion inertial length.

5. Discussion and Conclusions

In the previous section, we have presented observations of four magnetic field structures as seen by the STAFF search coil magnetometer on the satellites Cluster 3 and Cluster 4 in the inner magnetosphere. These instances are not unique. Bipolar signatures, characterized by two, closely spaced peaks in the field magnitude surrounding a central field minimum associated with a large, rapid field rotation were observed in the STAFF continuous waveform burst science data were observed in a number of BM data periods. A quick survey of 3 h of Cluster 3 waveform data captured on November 14, 2018 appears to contain over 100 structures.

To our knowledge, observations of such structures have not been previously reported within the inner magnetosphere. The twin/multipeaked structure of the magnetic field would rule out the possibility that these structures are some forms of flux rope. The fact that they do not appear to be associated with a bi/multipolar signature in the electric field would indicate that they are probably not related to ion or electron phase space holes although the field fluctuation associated with a phase space hole has similarities to the changes in magnetic field reported here. The fact that the background magnetic field, measured by FGM, shows little or no variation across the structure and the profile of the spacecraft potential does not show any change during an event compared to that measured before or after the event would indicate that there are no associated changes in the plasma density that would be expected if the structure is related to a mirror mode oscillation.

5.1. Physical Interpretation

These structures, observed primarily in the STAFF-SC magnetometer, appear to be some form of filamentary structure containing a strong magnetic field gradient across them. This field gradient would give rise to a current flowing along the structure. Since the WBD and EFW data show no evidence for changes in the electric field or spacecraft potential within the BMS, it is assumed that the displacement current term $\partial\mathbf{E}/\partial t = 0$ and so the magnitude of this current can be estimated using

$$\mathbf{V} \times \mathbf{B} = \mu_0 \mathbf{J} \tag{1}$$

where **B**, and **J** are the magnetic flux density, and current, respectively, μ_0 is the permeability of free space. If the structure is indeed a current filament, then its axis will lie along the minimum variance direction and the magnetic field gradient across the center of the structure can be estimated from the maximum and intermediate variance components. Based on these assumptions, the current density was estimated to be of the order of 10–40 $\mathrm{nA\,m^{-2}}$.

From the analysis presented in Sections 4.1 and 4.2 above, it was determined that the variance frames determined from the individual satellite observations of an BMS differ considerably. This result would be expected if the event studied were nonplanar. It was speculated that the BMS may result from the satellites encountering a current filament.

From Ampere's Law, the current filament will have an associated magnetic field in the plane perpendicular to the flow direction that will perturb the background magnetic field. This field perturbation was investigated using a simplified current model based on the assumption that the current filament may be represented as an infinitely long conductor of radius R along which a current I flows. In such a case, the magnetic flux density B of this perturbation at a distance r from the axis of the filament is given by

$$B = \begin{cases} \dfrac{\mu_0 I r}{2\pi R^2} & \text{if } r <= R \\ \dfrac{\mu_0 I}{2\pi r} & \text{if } r > R \end{cases}$$

Figure 8 shows the magnetic field profiles that would be expected to be observed by a satellite traveling in the plane perpendicular to the direction of current flow (assumed to be along the Z direction). In Panel (a) the black circles represent the extent of the two concentric regions that carry currents along the +Z (inner solid) and −Z (outer dashed) directions. Both current cylinders carry the same current, however, their current densities will differ due to the differing cross-sectional areas of the current cylinders. The red, green, blue, magenta, and cyan lines show the simulated satellite trajectories. The red, magenta, and cyan trajectories pass through the axis of the current cylinder while the red and green trajectories pass on opposite sides of the axis of the current cylinder. Panels (b–d) show the expected magnetic field magnitude, X-component, and Y-component, respectively, with colors corresponding to the various trajectories. The vertical black lines indicate the extent of the inner (solid) and outer (dashed) current regions. Note that some of the curves plotted may be partly obscured.

The red and cyan trajectories pass through the current cylinder in directions that are perpendicular (panel a). As expected, the field magnitudes due to the current cylinders are identical, with only the cyan trajectory visible in panel (b). The field components of these trajectories, shown in panels (c) and (d) also show similarities in that they exhibit a bipolar signature in which the field shows a negative peak followed by a positive one (or vice versa). In the case of the B_Y component, both profiles are identical whereas the B_X components are mirror images of each other. Thus, when comparing twin satellite measurements such as those shown in Figures 6 and 7 it appears that in the former case the satellite trajectories are virtually parallel with respect to the current cylinder while in the latter case, with the oppositely directed B_Y field profiles, the trajectories are almost perpendicular with respect to the current cylinder. This behavior is indicative of the temporal or spatial evolution of the current cylinder occurring between the twin spacecraft observations. The magenta trajectory shows a cut through the BMS parallel to the X axis. Its magnitude is identical to the red and cyan trajectories and the components show that, as expected, the field is directed in the Y direction. These trajectories also show that the magnitude maxima mark the limits of the size of the inner current region and that the size of the outer current region is defined by the points at which the magnitude begins

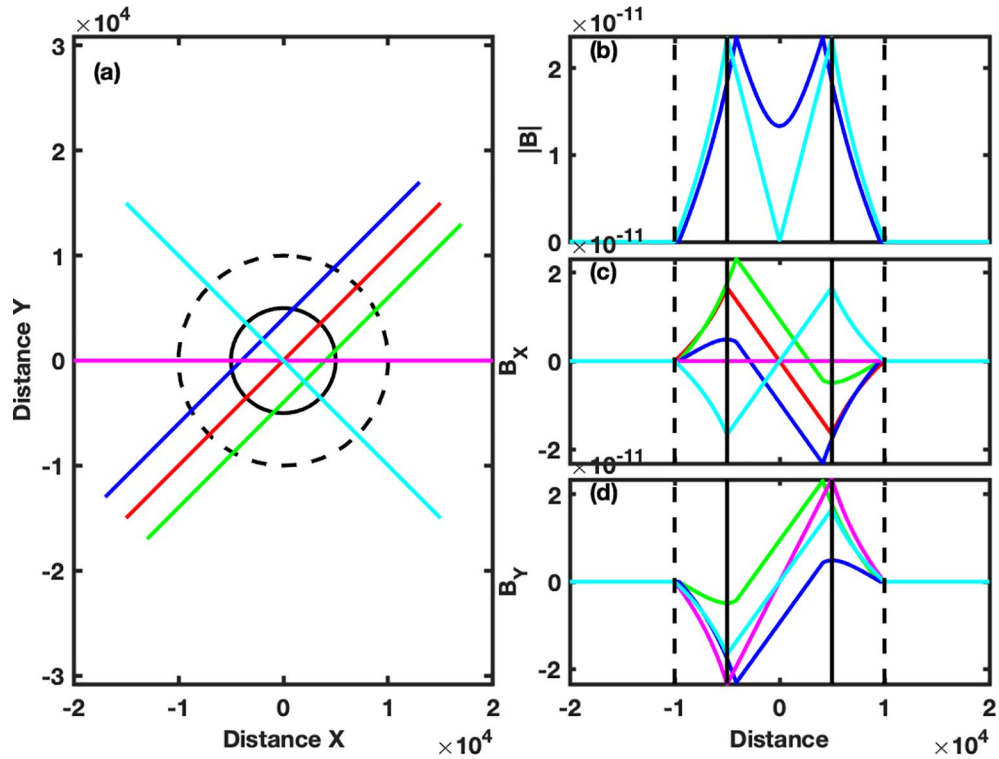

Figure 8. A comparison of profiles of the magnetic field magnitude for different combinations of the current and the cylinder radius in which it is confined. The model current densities used were 1e−8 nA m^{-2} and −0.25e−8 nA m^{-2} for the inner and outer current regions.

to grow and the beginning on the field rotation. The field profiles along the trajectories that pass through the axis of the current cylinders, are very similar to those observed in events with large amplitudes. Outside of the current cylinders the contribution to the observed field is zero, since the fields created by the individual, opposing currents cancel each other at distances beyond the outer boundary of the larger current cylinder.

The blue and green trajectories are parallel to the red, and are offset so that they do not pass through the center of the current cylinder. Such trajectories are characterized by a central field minimum that does not approach zero magnitude. It should be noted that in the search for BMS events, field profiles such as these would not have been selected, resulting in a bias in the selection of events that favors current cylinder crossings in which the satellite trajectory passes close to the central axis of the cylinder.

5.2. Analysis of Possible Calibration Effects

While BMS observations may be due to an encounter with a current filament, it should also be noted that calibration procedure applied to the raw data could also contribute to the overall profile of the event. As was mentioned in Section 2, the 450 Hz sampled STAFF-SC continuous waveform data in GSE coordinates covers the frequency range 0.6–180 Hz. This frequency range results from two filtering processes. First, a low pass 180 Hz filter was applied to the sampled data onboard prior to digitization. Second, the ground-based calibration process of the GSE data set employs a high-pass 0.6 Hz filter to considerably reduce any residual spin tone interference that would otherwise be present in this data set. Figure 9 shows a comparison of the idealized field profile due to a cylindrical current element (red curves) and a simulation of the sampling and application of a high-pass filter to these measurements (blue curves). It is seen that the application of the high-pass filter changes the $1/r$ decay in the field profile outside of the idealized current cylinder, causing a steeper decay profile to be observed in the data and also adding a ringing effect to the signal as evidenced by the small oscillations in field profile observed either side of the main peaks. Some of the events shown in this paper do indeed show evidence of this ringing effect. The potential effects of this high-pass filtering

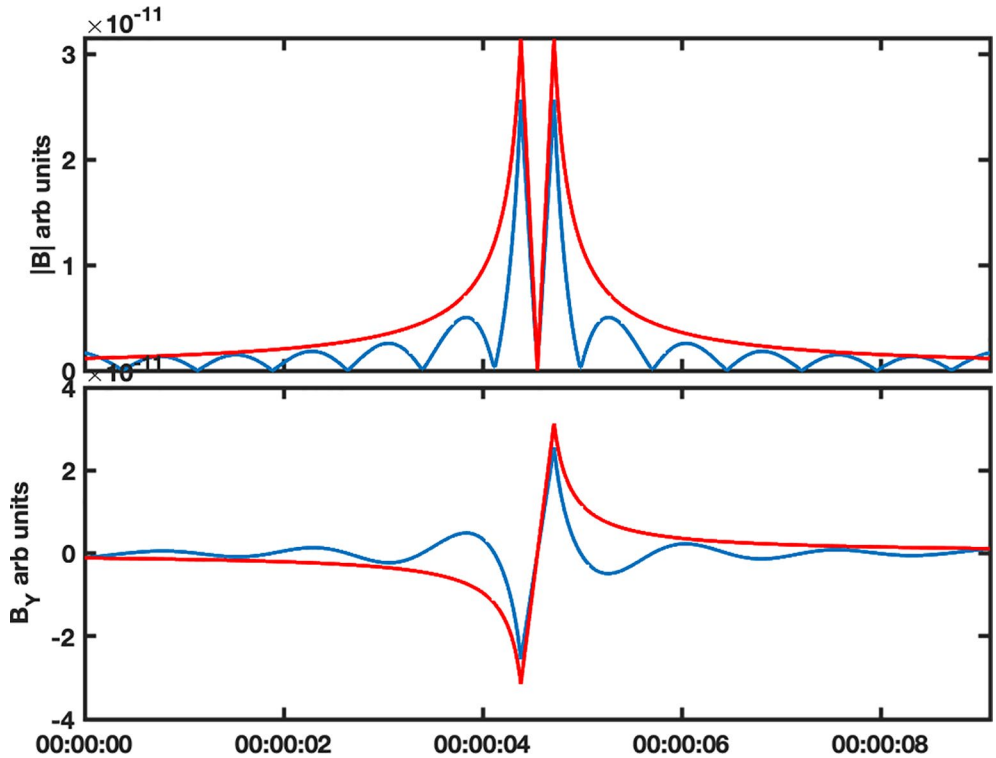

Figure 9. A comparison of the idealized current profile based on the above equations (red) and the profile seen in the STAFF-SC CWF GSE data set that has been high-pass filtered (blue).

applied during the calibration process were investigated further using various filter cut-off frequencies and FFT sizes. The results indicated that these effects had minimal influence on the field gradients observed in the data set. The striking observation about these events, which does not depend much on the calibration, is the sharp change in the field gradient at the edge of the central core. This implies that the current filaments have a uniform current density inside, with a sharp edge.

To summarize, in this report we have presented observations of bipeaked structures in the magnitude of the magnetic field observed by the Cluster STAFF-SC instruments.

Using simple models of the magnetic field induced by an infinite current cylinder, we argue that the resulting magnetic profiles are the result of encounters with small-scale current filaments.

Future studies will aim to determine the locations in which these structures are observed and include a statistical investigation to determine their general properties such as size, orientation, and look more fully into their propagation.

Conflict of Interest

The authors declare no conflicts of interest relevant to this study.

Data Availability Statement

The data used in this study were obtained from the Cluster Science Archive (https://csa.esac.esa.int/csa-web/).

Acknowledgments
Simon N. Walker and Michael A. Balikhin were supported by funding from the UK STFC ST/R000697/1. Patrick Canu thanks CNES for support in Staff operations and data processing. Michael A. Balikhin is grateful to A. Artemyev for very useful discussions. Simon N. Walker wishes to thank I. Dandouras for useful advice regarding the interpretation of the CIS data.

References

Aryan, H., Walker, S. N., Balikhin, M. A., & Yearby, K. H. (2019). Equatorial magnetosonic waves observed by cluster satellites: The Chirikov resonance overlap criterion. *Journal of Geophysical Research: Space Physics*, *124*, 2864–2872. https://doi.org/10.1029/2019JA026680

Balikhin, M. A., Shprits, Y. Y., Walker, S. N., Chen, L., Cornilleau-Wehrlin, N., Dandouras, I., et al. (2015). Observations of discrete harmonics emerging from equatorial noise. *Nature Communications*, *6*, 7703. https://doi.org/10.1038/ncomms8703

Balogh, A., Dunlop, M. W., Cowley, S. W. H., Southwood, D. J., Thomlinson, J. G., Glassmeier, K. H., et al. (1997). The Cluster magnetic field investigation. *Space Science Reviews*, *79*, 65–91. https://doi.org/10.1023/A:1004970907748

Cornilleau-Wehrlin, N., Chauveau, P., Louis, S., Meyer, A., Nappa, J. M., Perraut, S., et al. (1997). The Cluster Spatio-Temporal Analysis of Field Fluctuations (STAFF) experiment. *Space Science Reviews*, *79*, 107–136. https://doi.org/10.1023/A:1004979209565

Décréau, P. M. E., Fergeau, P., Krannosels'kikh, V., Leveque, M., Martin, P., Randriamboarison, O., et al. (1997). WHISPER, a resonance sounder and wave analyser: Performances and perspectives for the Cluster mission. *Space Science Reviews*, *79*, 157–193. https://doi.org/10.1023/A:1004931326404

Escoubet, C. P., Schmidt, R., & Goldstein, M. L. (1997). Cluster—Science and mission overview. *Space Science Reviews*, *79*, 11–32. https://doi.org/10.1023/A:1004923124586

Gurnett, D. A., Huff, R. L., & Kirchner, D. L. (1997). The wide-band plasma wave investigation. *Space Science Reviews*, *79*, 195–208. https://doi.org/10.1023/A:1004966823678

Gustafsson, G., Boström, R., Holback, B., Holmgren, G., Lundgren, A., Stasiewicz, K., et al. (1997). The Electric Field and Wave experiment for the Cluster mission. *Space Science Reviews*, *79*, 137–156. https://doi.org/10.1023/A:1004975108657

Khrabrov, A. V., & Sonnerup, B. U. Ö. (1998). Error estimates for minimum variance analysis. *Journal of Geophysical Research*, *103*, 6641–6651. https://doi.org/10.1029/97JA03731

Shklyar, D. R., & Balikhin, M. A. (2017). Whistler mode waves below lower hybrid resonance frequency: Generation and spectral features. *Journal of Geophysical Research: Space Physics*, *122*, 10072–10083. https://doi.org/10.1002/2017JA024416

Sonnerup, B. U. Ö., & Cahill, L. J., Jr. (1967). Magnetopause structure and attitude from explorer 12 observations. *Journal of Geophysical Research*, *72*, 171–183. https://doi.org/10.1029/JZ072i001p00171

Walker, S. N., Balikhin, M. A., Shklyar, D. R., Yearby, K. H., Canu, P., Carr, C. M., & Dandouras, I. (2015). Experimental determination of the dispersion relation of magnetosonic waves. *Journal of Geophysical Research: Space Physics*, *120*, 9632–9650. https://doi.org/10.1002/2015JA021746

Woolliscroft, L. J. C., Alleyne, H. S., Dunford, C. M., Sumner, A., Thompson, J. A., Walker, S. N., et al. (1997). The digital wave-processing experiment on cluster. *Space Science Reviews*, *79*(1–2), 209–231. https://doi.org/10.1023/A:1004914211866